

**Supplementary Information**

**Performance of a Mixing Entropy Battery  
Alternately Flushed with Wastewater Effluent and  
Seawater for Recovery of Salinity-gradient Energy**

Meng Ye,<sup>ad</sup> Mauro Pasta,<sup>b</sup> Xing Xie,<sup>ab</sup> Yi Cui,<sup>bc\*</sup> Craig S. Criddle<sup>\*ad</sup>

<sup>a</sup>*Department of Civil and Environmental Engineering, Stanford University, Stanford, California  
94305, USA.*

<sup>b</sup>*Department of Materials Science and Engineering, Stanford University, Stanford, California 94305,  
USA.*

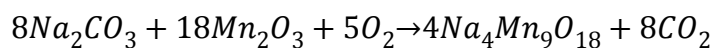
<sup>c</sup>*Stanford Institute for Materials and Energy Sciences, SLAC National Accelerator Laboratory, Menlo  
Park, California 94025, USA.*

<sup>d</sup>*Woods Institute for the Environment and the Department of Civil and Environmental Engineering,  
Stanford University, Stanford, California 94305, USA.*

\*To whom correspondence should be addressed. E-mail: [ccriddle@stanford.edu](mailto:ccriddle@stanford.edu)

**Synthesis of sodium manganese oxide (NMO)**

The NMO powder was synthesized by the solid-state reaction<sup>S1</sup>:



The precursor powders were mixed with Na:Mn molar ratio of 0.44 then heated in air in a Lindberg Moldatherm Box Furnace (Fisher Scientific) at a rate of 20 °C/min to 300 °C, held at 300°C for 2 hours, then heated at a rate of 20 °C/min to 800 °C. This temperature was held constant for 12 hours, and the sample cooled was then cool to room temperature<sup>S1</sup>. Fig. S1 illustrates the SEM image of the sample. .

**Fabrication and pre-cycle of electrodes**

1 The NMO and Ag electrodes were prepared through an ink coating process followed  
2 by electrochemical pre-cycle. The ink was prepared by mixing synthesized NMO (85%  
3 wt.) or silver nanoparticles (85% wt.) with Super-P (TIMCAL, 8% wt.) and PVDF (7%  
4 wt.). N-methyl pyrrolidone (NMP) was added to the mixture as solvent, and the ink  
5 was stirred overnight before using<sup>S2</sup>. Carbon cloth (3cm×3cm) was used as the current  
6 collector. The electrodes were prepared by coating NMO or Ag ink onto carbon cloth  
7 then dried in a vacuum for 24 hours. The loading of active materials was ~14mg/cm<sup>2</sup>.  
8 As shown in Fig. S2, the oxidation and reduction of NMO electrodes involved two  
9 voltage plateaus. The NMO electrode was pre-oxidized in 0.6M NaCl solution to the  
10 beginning of a 0.3 V voltage plateau where experiments were conducted. As shown in  
11 Fig. S3, the Ag electrode was also pre-cycled in 0.6 M NaCl solution to oxide part of  
12 the Ag to AgCl. The measured potential of 0.045 V vs. Ag/AgCl (3.5 M KCl)  
13 indicates that the reaction at the silver electrode is dominated by interaction with  
14 chloride ions.

## 15 **Electrochemical properties of NMO**

16 As the cycle time increased to 20 hours (Fig. S4) the slope of voltage-charge curve  
17 increased, and the charge curve crossed the discharge curve. Appreciable energy loss  
18 resulted. These losses were attributed to transitions between voltage plateaus. For  
19 NMO, two voltage plateaus were observed during the charge/discharge cycle (Fig.  
20 S2). The transitions between plateaus were irreversible and resulted in energy losses.  
21 To prevent these losses, the charge/discharge cycle was maintained at a lower plateau

1 (0.3 V in this case). When operated at a voltage above the plateau transition, the  
 2 voltage ratio decreased from >80% to 22%, and overall energy recovery was just 0.08  
 3 kWh/m<sup>3</sup>. To avoid this loss with NMO electrodes, the voltage was maintained within  
 4 the 0.3 V plateau. For these conditions,, the utilized specific capacity was only ~1/3  
 5 of the total NMO specific capacity of 35 mAh/g. These results underscore the need  
 6 for new cationic electrode materials.

### 7 **Derivation of Theoretically Extractable Energy from Mixing**

8 The theoretically extractable energy is:

$$9 \quad \Delta G_{mix} = 2RT[V_E C_E \ln \frac{C_E}{C_M} + V_S C_S \ln \frac{C_S}{C_M}]$$

10 where the first term inside the parentheses is the work required for salination of the  
 11 wastewater effluent, and the second term is the work required for dilution of the  
 12 seawater. The coefficient 2 reflects the product of the anion and cation  
 13 concentrations, where these values must be equal to maintain a charge balance.  $C_E$  is  
 14 the NaCl concentration in the wastewater effluent (0.032 M, in this study);  $C_S$  the  
 15 NaCl concentration in seawater (0.6 M);  $V_E$  the volume of wastewater effluent;  $V_S$  the  
 16 volume of seawater;  $R$  the universal gas constant; and  $T$  the absolute temperature.  $C_M$   
 17 is the NaCl concentration after complete mixing of wastewater effluent and seawater:

$$18 \quad C_M = \frac{V_E C_E + V_S C_S}{V_E + V_S}$$

19 As shown in Fig. S5, when the volume of wastewater effluent is fixed, the available  
 20 free energy increases with the volume ratio between seawater and wastewater effluent.  
 21 The maximum available free energy approaches ~0.65kWh/m<sup>3</sup> as the volume ratio  
 22 approaches infinity.

## 1 Calculation of Theoretical Voltage Rise

2 We used the Nernst equation to calculate the voltage rise for the following reaction:



4 The computed voltage rise is:

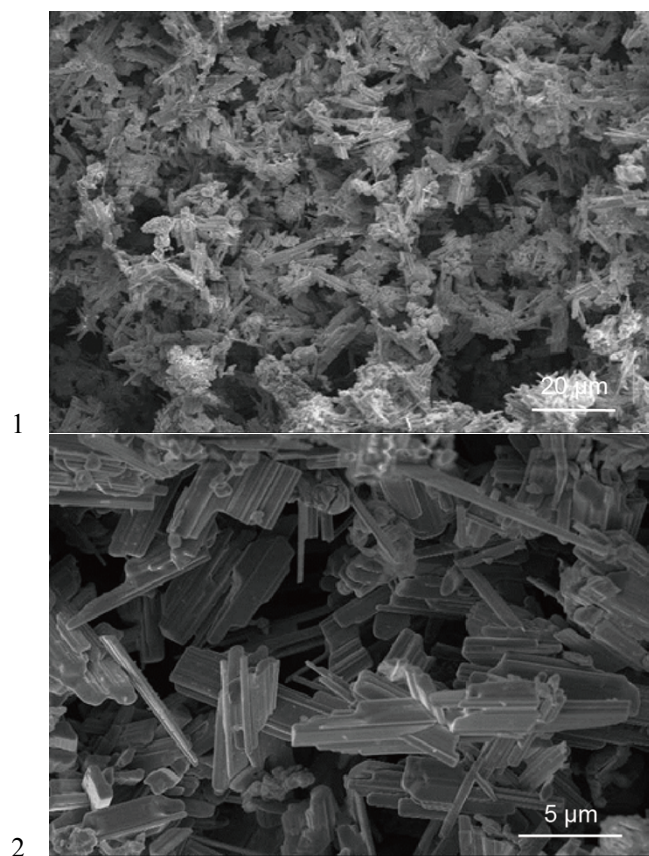
5 
$$\Delta E = \frac{RT}{zF} \ln \left( \frac{c_{\text{Na}^+, \text{seawater}} \cdot c_{\text{Cl}^-, \text{seawater}}}{c_{\text{Na}^+, \text{wastewater}} \cdot c_{\text{Cl}^-, \text{wastewater}}} \right)^4$$

6 where  $z$  is the number of moles of electrons transferred in the cell reaction,  $F$  the  
7 Faraday constant,  $R$  the universal gas constant, and  $T$  the absolute temperature. In this  
8 study, the concentrations of  $\text{Na}^+$  and  $\text{Cl}^-$  are each equal to 0.6 M in seawater and  
9 0.032 M in wastewater effluent. The computed voltage rise when changing the  
10 solution from wastewater effluent to seawater is 0.151 V. In the operation of MEBs,  
11 the wastewater effluent becomes more saline after the charge step, so the voltage rise  
12 is calculated using the concentrations of  $\text{Na}^+$  and  $\text{Cl}^-$  in the wastewater effluent after  
13 the charge step (denominator of the above equation) and the numerator is the the  
14 concentrations of  $\text{Na}^+$  and  $\text{Cl}^-$  in the seawater.

## 15 References

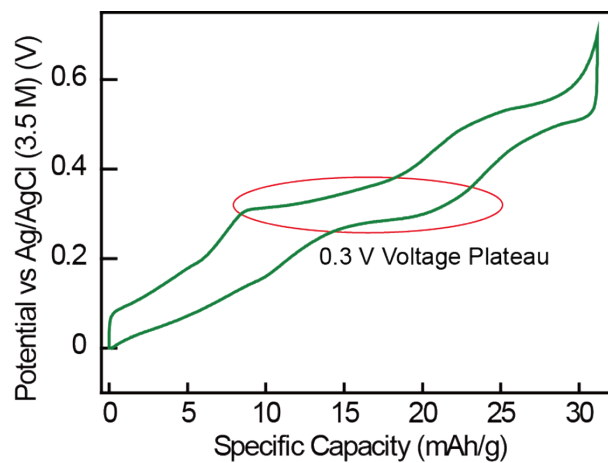
- 16 S1 D. Tevar, J. F. Whitacre, *Journal of The Electrochemical Society*, 2010, **157**,  
17 A870.
- 18 S2 F. La Mantia, M. Pasta, H. D. Deshazer, B. E. Logan, Y. Cui, *Nano Lett.*, 2011,  
19 **11**, 1810.

## 20 Supplementary figures



3 **Figure S1** Scanning electron microscope (SEM) image of the  $\text{Na}_4\text{Mn}_9\text{O}_{18}$  powder  
4 showing the nanorod morphology.

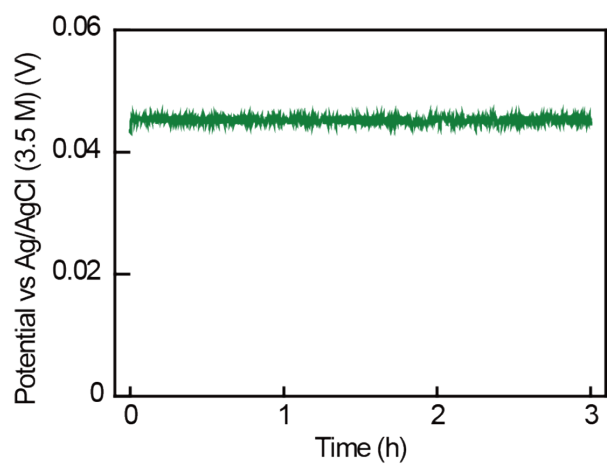
5



1

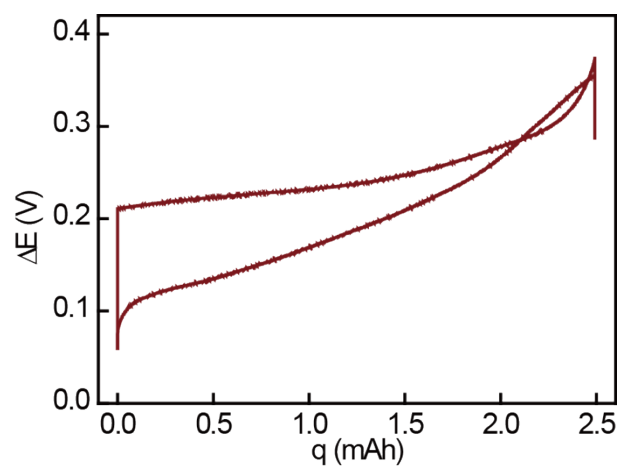
2 **Figure S2** Galvanostatic (1mA) cycles of  $\text{Na}_4\text{Mn}_9\text{O}_{18}$  electrode.

3



4

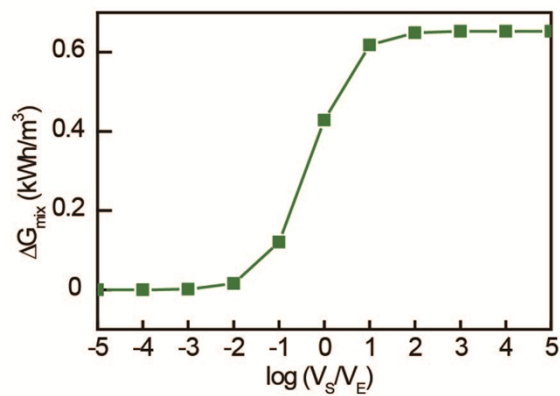
5 **Figure S3** Pre-cycle of Ag/AgCl electrode.



6

7 **Figure S4** Plot of  $\Delta E$  vs.  $q$  showing energy extraction at cycle times of 20 h.

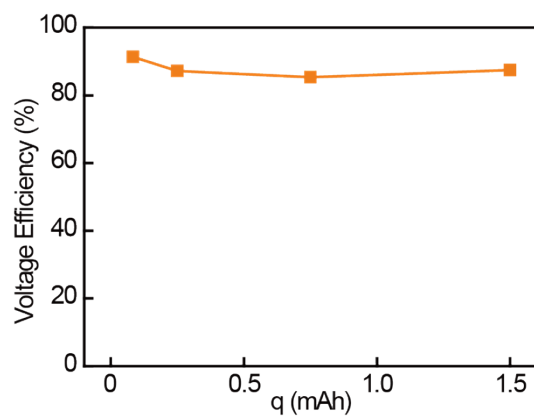
1



2

3 **Figure S5** Plot of theoretically extractable energy vs. logarithm of mixing ratio.

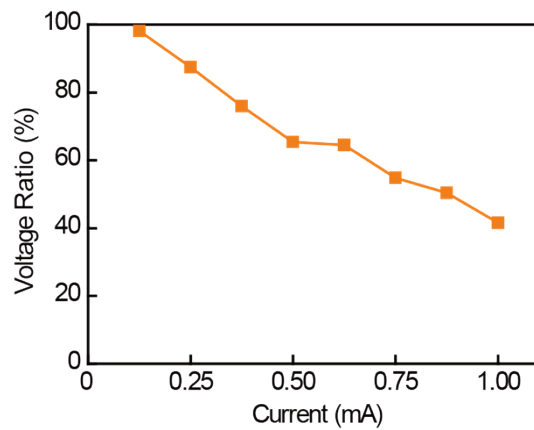
4



5

6 **Figure S6** Voltage ratio of each cycle with different cycle time.

7

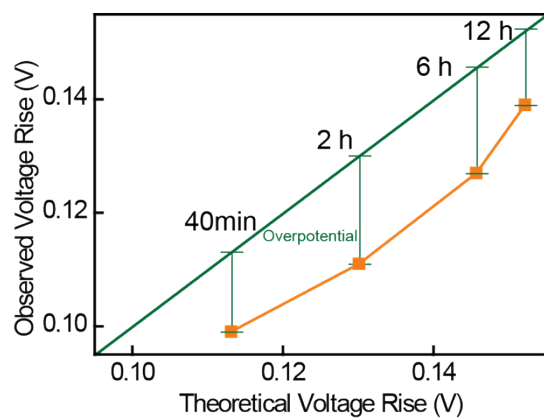


8

9 **Figure S7** Voltage ratio of each cycle at different applied currents.

1

2



3

4 **Figure S8** Observed voltage rise vs. theoretical voltage rise with different cycle time:

5 the orange line shows the observed voltage rise with different cycle time. The

6 difference between the ideal voltage (straight line) and the actual voltage (curved line

7 with squares) represents the overpotentials in different scenarios.

8